Indian Journal of Pure & Applied Physics
Vol. 54, April 2016, pp. 263-268

Magnetic field induced bandgap in two dimensional magneto-optical photonic crystals

Z H Yu, P Yu, B H Yin & Z Y Wang*
Ningbo Institute of Technology, Zhejiang University, Ningbo, China

Received 14 January 2014; revised 27 January 2015; accepted 21 May 2015

The photonic bandgap of magneto-optical (MO) photonic crystals (PhCs) induced by an external dc magnetic field is theoretically investigated with the plane-wave expansion method. The effect of PhC lattice shape, MO filling fraction and dc magnetic intensity on such type of bandgap has been studied. It is found that PhC with triangular lattice is superior to PhC with square lattice in term of bandgap width; thus, the one-way waveguide composed by the former PhC has a broader operation band. Moreover, there exists a certain value of external magnetic field at which the bandgap reaches a maximum. These results are found to be in agreement by finite element analysis of transmission property of one-way waveguides.

Keywords: Photonic bandgap, Magneto-optical (MO) photonic crystal, Photonic crystal lattice shape, Magnetic intensity

1 Introduction

The ability to control light propagation dynamically using photonic crystals (PhCs) has been demonstrated both theoretically and experimentally in recent years[1-8]. To influence the light-matter interaction, the refractive index in a PhC is generally periodically modulated by properly arranging the PhC's structure and its parameters. As a result, the interferences of electromagnetic (EM) waves scattering from unit cells make the frequencies in a certain range be strongly rejected by the structure. That is, lights of some frequencies cannot propagate through the structure, while lights of other frequencies can be transmitted. Such a phenomenon is called photonic bandgap[9] (PBG). PhCs have been used in design of a great deal of devices, such as waveguides[4,8,10-12], optical fibers[6,7,13], resonant[14], filters[15] and splitters[16].

Reflection in optical devices may cause severe problems in practice. For example, the reflection from nearby structures of the emitted light may make the operation of laser diodes unstable. In conventional PhCs circuits, however, reflection may become inevitable at sharp waveguide bends and/or the connection of two components. To avoid the problems caused by reflection, researchers have proposed several concepts for realizing unidirectional transmission recently. Figotin and Vitebskiy[17,18] used the "frozen mode" to achieve unidirectional transmission, where the group velocity of the reflected waves is zero. More recently, Wang[19,20] proposed the concept of one-way mode, where no reflected wave presents in the device. The one-way mode provides a new way to control the behaviour of EM waves in PhCs, making it possible to create new classes of photonic devices.

The sufficient condition to ensure the one-way mode is to break the spectral symmetry and time-reversal symmetry in PhCs. The commonly used approaches to achieve one-way mode are based on the anisotropic materials[19,21] (e.g. magneto-optical materials) or nonlinear materials[22]. Recently, the one-way PhC guiding system based on the MO materials attracted a great deal of attention and their advantages have been demonstrated both theoretically and experimentally[19-21,23-27]. Under an external magnetic field, the magneto-optical (MO) materials possess a permittivity or permeability tensor with non-zero imaginary off-diagonal elements. Thus, the media is gyro-electric or gyro-magnetic anisotropic and simultaneously breaks the time-reversal symmetry.

As a kind of most basic but useful components in photonic devices, waveguides supporting one-way mode (i.e. one-way waveguides) have been proposed by many researchers[20,21]. In a MO PhC, the one-way waveguide is often formed by the interface between the MO PhC and a cladding, supporting non-bulk

*Corresponding author (E-mail:zaihe.yu@nit.zju.edu.cn)

modes in the frequency range of the MO PhC bandgaps, where the cladding can be selected as a metal slab, a regular PhC or a MO PhC with opposite external magnetic field. This PhC bandgap must be such a type that it is induced by an external magnetic field breaking the time-reversal symmetry of the system, and it also, generally, determines the band width of the one-way mode. Therefore, it is necessary to study the property of such special bandgap of MO PhCs. It was reported that the applied external magnetic field influenced the band gap of one-dimensional[28,29] (1D) MO PhCs (in infrared range). The MO material included in these 1D MO PhCs only has a weak MO effect with the gyration far smaller than 1. The band gap of these 1D PhC exists even in the absence of the external magnetic field, which is quite different from what is employed in the one-way PhC waveguides.

In the present paper, the band structures of MO PhCs, with two-dimensional square and triangular lattices under an external magnetic field applied, have been investigated. The analyzed PhCs are of dielectric-air structure (i.e. long parallel of dielectric rods in air) and the rods are of yttrium-iron-garnet material. For both structures, the plane-wave expansion method is applied to analyze the influence of the lattice type, filling fraction (i.e. radius of the rods) and the intensity of the external dc magnetic field on the external-magnetic-field induced bandgap. The simulated results are verified through finite element analysis of one-way waveguides composed by MO PhCs.

2 Band Structure Calculation

From Maxwell's equations, the master equation governing the propagation of EM waves in a MO PhC can be expressed as:

$$\nabla\times[\mu(\boldsymbol{r})^{-1}\nabla\times\boldsymbol{E}]=\varepsilon(\boldsymbol{r})\ {}^{2}\boldsymbol{E} \qquad \ldots (1)$$

where, , is the mode frequency; and ($\boldsymbol{r}$) and ($\boldsymbol{r}$), the permeability tensor and the scalar permittivity at position $\boldsymbol{r}$, respectively. Since the permeability tensor is taken into account and both the inverse permeability tensor and the scalar permittivity ε(r) are functions of position $\boldsymbol{r}$, Eq. (1) is different from the usual master equation of PhCs.

The two-dimensional MO PhCs and the E-polarization waves are considered. The MO material in the PhCs is assumed to be yttrium-iron-garnet (YIG). When an external dc magnetic field $\boldsymbol{H}_0$ is applied along the out-of-plane direction (i.e. z direction), the permeability of the YIG will have the following gyro-magnetic form:

$$\mu(\mathrm{r}) = {}_{0}\begin{bmatrix} & \boldsymbol{ik} & 0 \\ -\boldsymbol{ik} & & 0 \\ 0 & 0 & 1 \end{bmatrix} \qquad \ldots (2)$$

where, $=1+\frac{\boldsymbol{m}\ {}_{0}}{({}^{2}_{0}-{}^{2})}$; $\boldsymbol{k}=\frac{-\ \boldsymbol{m}}{({}^{2}_{0}-{}^{2}]}$;

${}_{0}=2\quad\boldsymbol{H}_0$; and ${}_{\boldsymbol{m}}=2\quad(4\ \boldsymbol{m}_{\mathrm{s}})$.

The material parameters for the YIG are $=2.8\times10^{6}$ and $4\ \boldsymbol{m}_{\mathrm{s}}=1780$.

In order to investigate the band diagrams of MO PhC, numerical calculation of Eq. (1) was performed using the plane wave expansion method[31] (PWEM). As only a narrow operation (frequency) range is of interest in the present study, which corresponds to the magnetic field induced bandgap, the material dispersion is neglected in the calculation for simplicity, i.e., constant permeability components in Eq. (2) are taken into account. For consistency, a proper value of the lattice constant of a MO PhC is chosen so that the band gap lies within the operation range. The simulation results for structures with square and triangular lattices are reported and discussed.

The MO PhC structure of square lattice as described by Wang[20,21] is the comparison benchmark used by many researchers. For this structure, when an external dc magnetic field of 1600 Oe is applied, the tensor elements[32] in Eq. (2) for YIG at 4.28 GHz are = 14 and = 12.4. The present simulations indicate that the range of rod radius supporting one-way mode bandgap is from 0.06 $\boldsymbol{a}$ to 0.16 $\boldsymbol{a}$, where $\boldsymbol{a}$ is the lattice constant of MO PhC. For the purpose of comparison, the band diagrams of this structure for radius $\boldsymbol{r}$ = 0.06 $\boldsymbol{a}$, 0.11 $\boldsymbol{a}$ and 0.13 $\boldsymbol{a}$ are shown in Fig. 1(a-c), respectively. Figure 1(d) shows the relationship between the rod radius and the bandgap width. It is evident that the rod radius has impact on the width of the magnetic field induced bandgap. For the simulated magnetic field intensity, the largest bandgap width [i. e. about 0.052($\boldsymbol{a}/2\ \boldsymbol{c}$)] is achieved at $\boldsymbol{r}$ = 0.1 $\boldsymbol{a}$.

For the structure with triangular lattice under the same external magnetic field, the calculated results show that the magnetic field induced bandgap only appears when the rod radius is between 0.065 ***a*** and 0.15 ***a***. This means that the range of radius supporting one-way mode for the triangular lattice is narrower than that for the square lattice. Figures 2 (a,b and c) show the band diagrams for the triangular lattice structure with rod radius of 0.07 ***a***, 0.1 ***a*** and 0.15 ***a***, respectively. Figure 2(d) shows the relationship between the rod radius and the bandgap width for the triangular lattice structure, where the largest bandgap width is achieved at ***r*** = 0.11 ***a***. By comparing Fig. 1(d) and Fig. 2(d), it can be concluded that the largest bandgap width for the triangular lattice structure is almost 1.5 times of that for the square lattice structure used by Wang[20,21]. That is, the structure with triangular lattice can provide wider band for one-way edge mode.

The effect of the external magnetic intensity on the magnetic field induced bandgap has also been investigated. In this numerical analysis, the angular frequency ( ) is fixed at 2 ∗3 GHz. The values of and ***k*** in Eq. (2) under different external magnetic intensities are calculated and shown in Fig. 3(a). The value of becomes negative for certain combinations of frequency and external magnetic intensity. This situation is out of concern in the present study and thus not discussed here. Figure 3(b) shows the simulation results for the normalized

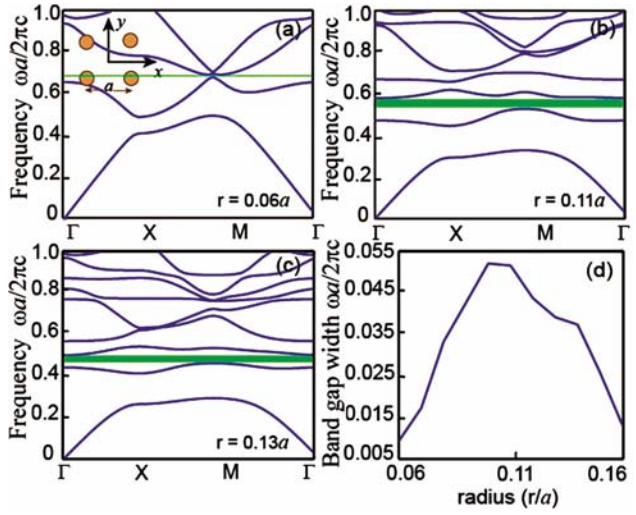

Fig. 1 – Band diagrams of MO PhC with square lattice of different radius values under dc magnetic field of 1600 Oe applied along the +z direction (= 14, = 12.4 at = 2 ∗4.28GHz) for radius ***r*** = (a) 0.06 ***a***, (b) 0.11 ***a*** and (c) 0.13 ***a***;. (d) relationship between rod radius and width of bandgap supporting one-way mode [***a*** is the lattice constant]

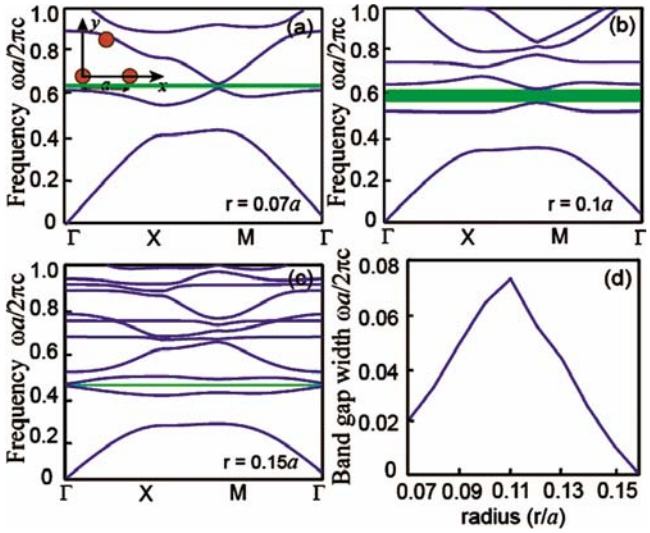

Fig. 2 – Band diagrams of MO PhC with triangular lattice of different radius values under ***dc*** magnetic field of 1600 Oe applied along the +z direction (= 14, = 12.4 at = 2 ∗4.28GHz) for radius ***r*** = (a) 0.07 ***a***, (b) 0.10 ***a*** and (c) 0.15***a***; (d) relationship between the rod radius and width of the bandgap supporting one-way mode [***a*** is lattice constant]

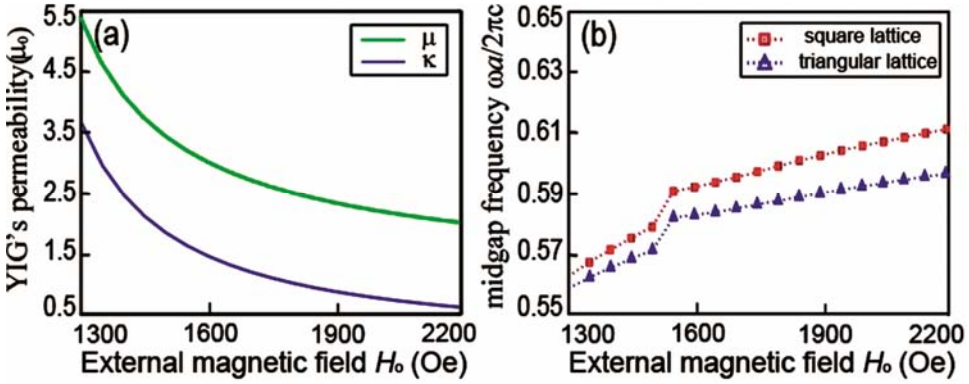

Fig. 3 – Impact of external magnetic intensity on the permeability of YIG and the bandgap of PhC at = 2 ∗3GHz (a) values of and in the permeability tensor for external magnetic intensity ranging from 1300 Oe to 2200 Oe and (b) midgap frequencies of the magnetic-field-induced bandgaps for MO PhCs with rod radius ***r*** = 0.11***a***

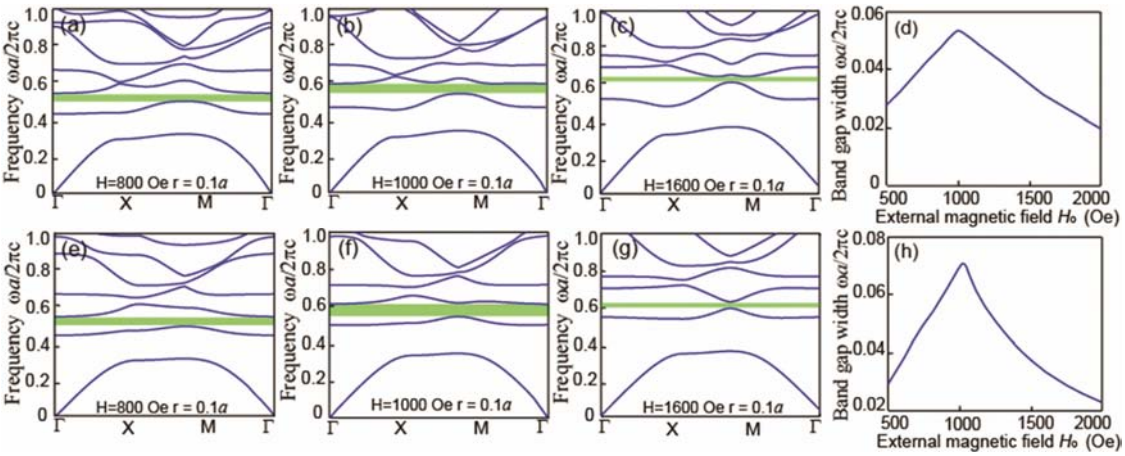

Fig. 4 – Band diagrams under different combinations of external ***dc*** magnetic intensity (denoted using ***H*** in the sub-figures) and YIG rod radius (***r***) at = 2 ∗3 GHz: (a-d) for square lattice PhC under ***H*** = (a) 800, (b) 1000, and (c) 1600 Oe, (d) relationship between bandgap width and YIG rod radius for PhC with square lattice under different external magnetic intensities; (e-h) for triangular lattice PhC under ***H*** = (e) 800, (f) 1000, and (g) 1600 Oe, (h) Relationship between bandgap width and YIG rod radius for PhC with triangular lattice under different external magnetic intensities

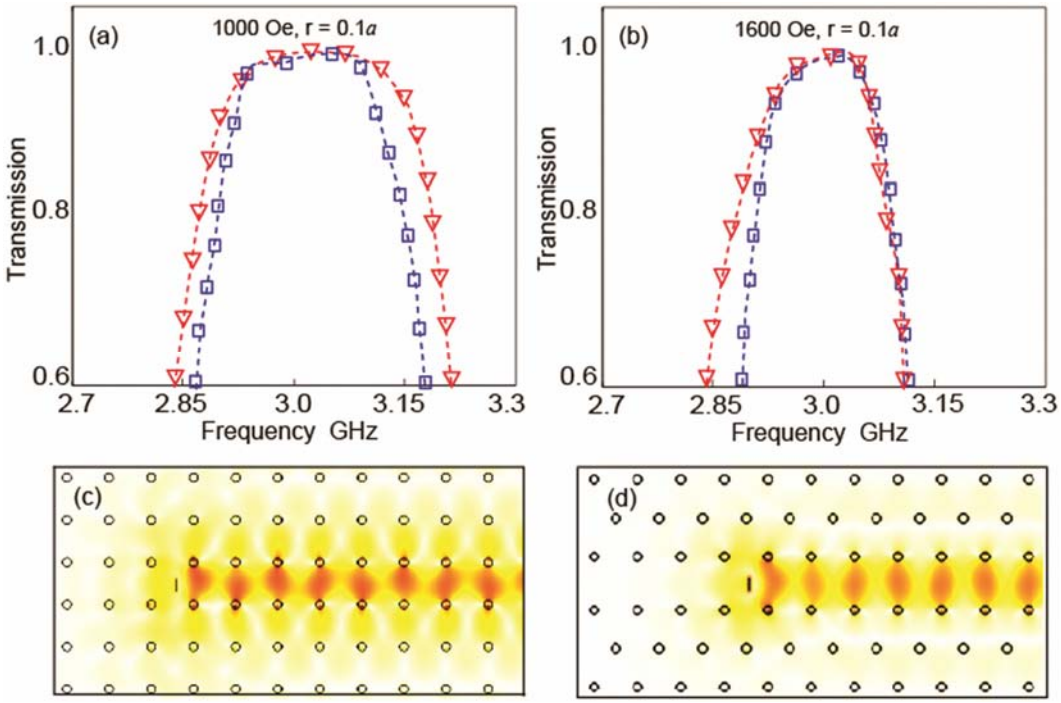

Fig. 5 – Simulation results for one-way waveguides composed by PhCs with square and triangular lattices: (a) Transmission properties of waveguides with different YIG PhC structures under ***H*** = 1000 Oe [curve with triangular marks is for waveguide with triangular lattice; curve with square marks is for waveguide with square lattice; and YIG rod radius is ***r*** = 0.1 ***a*** for both PhCs]; (b) transmission properties of waveguides with different YIG PhC structures under ***H*** = 1600 Oe; Simulated electric-field amplitudes for one-way waveguides with ***H*** = 1000 Oe at the frequency of 3 GHz with (c) square lattice and (d) triangular lattice

midgap frequency of the magnetic field induced bandgap. It is evident that the normalized midgap frequencies for both square lattice MO PhC and triangular lattice MO PhC exhibit piecewise linear and increasing relationship with respect to the external magnetic intensity. Moreover, the normalized midgap frequency of PhC with square lattice is always higher than that with triangular lattice and correspondingly, the former PhC has a larger lattice constant. The influence of the external magnetic intensity on the bandgap width is shown in Figs 4(a-h). For both types of PhC structures, the

bandgap width increases when the external magnetic field grows, but it reaches a maximum at a certain value of the external magnetic field and then decreases when the external magnetic field further grows. So, for one-way waveguide system, it is not true that the stronger the external magnetic field, the better it exhibits.

To confirm the above results, the finite element method[30] is applied to analyze the transmission features of one-way waveguides composed by 2-D PhCs with square and triangular lattices. Each 2-D PhC under study has a two-layered structure, and two external dc magnetic fields with identical magnetic intensity applied along the $+\boldsymbol{z}$ and $-\boldsymbol{z}$ axes, respectively to produce gyro-magnetic effect. This is similar to the one obtained earlier[16]. For the 2-D PhC with square (triangular) lattice, both the upper-layered and the lower-layered PhCs are a square (triangular) array of YIG rods ($=15$ $_0$)in air. The transmission features for the one-way waveguides with different structures under different magnetic fields are shown in Fig. 5. Figures 5(a and b) show the comparison of the PhC structure's impact on the one-way waveguide transmission, where the curve with triangular marks corresponds to the results for the waveguide, with triangular lattice. The curve with square marks shows the results for the waveguide with square lattice, and both the external magnetic intensity and the normalized value of rod radius ($\boldsymbol{r}/\boldsymbol{a}$) are the same for the two PhCs. The simulated electric field amplitudes for one-way waveguides with square and triangular lattices at 3 GHz are shown in Figs 5(c and d), where the external magnetic field is $\boldsymbol{H}_0 = 1000$ Oe. By carefully examining the results in Fig. 5, it can be concluded that the simulation results coincide with the results obtained using PWEM.

3 Conclusions

The effect of several factors on the magnetic field induced bandgap of MO PhCs that support one-way edge modes has been investigated. For PhCs with the same filling fraction and external magnetic intensity, the one with triangular lattice can provide wider band for one-way waveguide than that with square lattice, and the midgap frequency for the former is always lower than that for the latter. Moreover, there exists a certain value of external magnetic field, at which this type of bandgap reaches a maximum. The above results have been validated by finite element analysis of 2-D one-way mode waveguides composed by PhCs with triangular lattice and square lattice under different design parameters. The results of this paper can be used to guide the design of photo electronic devices such as waveguides, circulators, splitters, and some phase compensating devices.

Acknowledgement

The authors acknowledge the support for this work by the National Natural Science Foundation of China (Grant No. 61372005 and 61405177), the Science Foundation of Zhejiang Province (Grant No. LY14F030013) and Natural Science Foundation of Ningbo (Grant No. 2013A610004 and 2014A610150).

References

1 John S, ***Phys Rev Lett***, 58 (1987) 2486.
2 Yablonovitch E, ***Phys Rev Lett***, 58 (1987) 2059.
3 Lin, S Y, Chow, E, Hietala, V, Villeneuve, P R & Joannopoulos, J D, ***Science***, 282 (1998) 274.
4 Cuesta F, Griol A, Martinez A & Marti J, ***IET Elect Lett***, 39 (2003) 455.
5 Wang X, Hu X, Li Y, Jia W, Xu C, Liu X & Zi J, ***Appl Phys Lett***, 80 (2002) 4291.
6 Knight J C, ***Nature***, 424 (2003) 847.
7 Russell P, ***Science***, 299 (2003) 358.
8 Hughes S, Ramunno L, Young J F & Sipe J E, ***Phys Rev Lett***, 94 (2005) 033903.
9 Yablonovitch E, ***J Opt Soc Am B***, 10 (1993) 283.
10 Combrié S, De Rossi A, Morvan L, Tonda S, Cassette S, Dolfi D & Talneau A, ***IET Elect Lett***, 42 (2006) 86.
11 Chutinan A & Noda S, ***Appl Phys Lett***, 75 (1999) 3739.
12 Noda S, Tomoda K, Yamamoto N & Chutinan A, ***Science***, 289 (2000) 604.
13 Knight J C, Birks T A, Russell P S J & Atkin D M, ***Opt Lett***, 21 (1996) 1547.
14 Akahane Y, Asano T, Song B S & Noda S, ***Nature***, 425 (2003) 944.
15 Lee Y L R, Chauraya A, Lockyer D S & Vardaxoglou J C, ***IEE Proc Optoelectron***, 147 (2000) 395.
16 Wang Z Y, Yu Z H, Zheng X D & Wang L, ***J Electromag Wave***, 26 (2012) 1476.
17 Figotin A & Vitebskiy I, ***Phys Rev B***, 67 (2003) 165210.
18 Figotin A & Vitebskiy I, ***J Magn Magn Mater***, 300 (2006) 117.
19 Wang Z, Chong Y, Joannopoulos J D & Solja˘cic´ M, ***Phys Rev Lett***, 100 (2008) 013905.
20 Wang Z, Chong Y, Joannopoulos J D & Solja˘cic´ M, ***Nature***, 461 (2009) 772.
21 Haldane F D M & Raghu S**, *Phys Rev Lett***, 100 (2008) 013904.
22 Scalora M, Dowling J P, Bowden C M & Bloemer M J, ***J Appl Phys***, 76 (1994) 2023.

23 Poo Y, Wu R X, Lin Z F, Yang Y & Chan C T, ***Phys Rev Lett***, 106 (2011) 093903.
24 Fu J X, Lian J & Li Z Y, ***Appl Phy Lett***, 97 (2010) 041112.
25 Wang Z Y, Shen L F, Zhang X M, Wang Y G, Yu Z H & Zheng X D, ***J Appl Phys***, 110 (2011) 043106.
26 Fu J X, Lian J, Liu R J, Gan L & Li Z Y, ***Appl Phy Lett***, 98 (2011) 211104.
27 He C, Chen X L & Lu M H, ***Appl Phy Lett***, 96 (2010) 111111.
28 Vasiliev M, Belotelov V I, Kalish A N, Kotov V A, Zvezdin A K & Alameh K, ***IEEE Trans Magn***, 42 (2006) 382.
29 Zvezdin A K & Belotelov V I, ***Eur Phys J B***, 37 (2004) 479.
30 Monk P, ***Finite element methods for Maxwell's equations*** (Oxford University Press, Oxford), 2003
31 Ho K M, C T Chan & C M Soukoulis, ***Phys Rev Lett***, 65 (1990) 3152.
32 Pozar D M, ***Microwave engineering*** (Wiley, New York), 1998.